Inorganic Chemistry

Article

pubs.acs.org/IC

DFT Dissection of the Reduction Step in H_2 Catalytic Production by [FeFe]-Hydrogenase-Inspired Models: Can the Bridging Hydride Become More Reactive Than the Terminal Isomer?

Giulia Filippi, Federica Arrigoni, Luca Bertini, Luca De Gioia, and Giuseppe Zampella*

Department of Biotechnologies and Biosciences, University of Milano-Bicocca, Piazza della Scienza 2, 20126 Milan, Italy

Supporting Information

ABSTRACT: Density functional theory has been used to study diiron dithiolates $[HFe_2(xdt)(PR_3)_n(CO)_{5-n}X]$ (n = 0, 2, 4; R = H, Me, Et; X = CH_3S^-, PMe_3, NHC = 1,3-dimethylimidazol-2-ylidene; xdt = adt, pdt; adt = azadithiolate; pdt = propanedithiolate). These species are related to the [FeFe]-hydrogenases catalyzing the $2H^+ + 2e^- \leftrightarrow H_2$ reaction. Our study is focused on the reduction step following protonation of the $Fe_2(SR)_2$ core. Fe(H)s detected in solution are terminal (t-H) and bridging (μ-H) hydrides. Although unstable versus μ-Hs, synthetic t-Hs feature milder reduction potentials than μ-Hs. Accordingly, attempts were previously made to hinder the isomerization of t-H to μ-H. Herein, we present another strategy: in place of preventing isomerization, μ-H could be made a stronger oxidant than t-H ($E^\circ_{\mu\text{-H}} > E^\circ_{\text{t-H}}$). The nature and number of PR_3 unusually affect $\Delta E^\circ_{\text{t-H}-\mu\text{-H}}$: $4PEt_3$ models feature a μ-H with a milder E° than t-H, whereas the $4PMe_3$ analogues behave oppositely. The correlation $\Delta E^\circ_{\text{t-H}-\mu\text{-H}} \leftrightarrow$ stereoelectronic features arises from the steric strain induced by bulky Et groups in $4PEt_3$ derivatives. One-electron reduction alleviates intramolecular repulsions only in μ-H species, which is reflected in the loss of bridging coordination. Conversely, in t-H, the strain is retained because a bridging CO holds together the Fe_2 core. That implies that $E^\circ_{\mu\text{-H}} > E^\circ_{\text{t-H}}$ in 4-PEt_3 species but not in $4PMe_3$ analogues. Also determinant to observe $E^\circ_{\mu\text{-H}} > E^\circ_{\text{t-H}}$ is the presence of a Fe apical σ-donor because its replacement with a CO yields $E^\circ_{\mu\text{-H}} < E^\circ_{\text{t-H}}$ even in $4PEt_3$ species. Variants with neutral NHC and PMe_3 in place of CH_3S^- still feature $E^\circ_{\mu\text{-H}} > E^\circ_{\text{t-H}}$. Replacing pdt with $(Hadt)^+$ lowers E° but yields $E^\circ_{\mu\text{-H}} < E^\circ_{\text{t-H}}$, indicating that μ-H activation can occur to the detriment of the overpotential increase. In conclusion, our results indicate that the electron richness of the Fe_2 core influences $\Delta E^\circ_{\text{t-H}-\mu\text{-H}}$, provided that (i) the R size of PR_3 must be greater than that of Me and (ii) an electron donor must be bound to Fe apically.

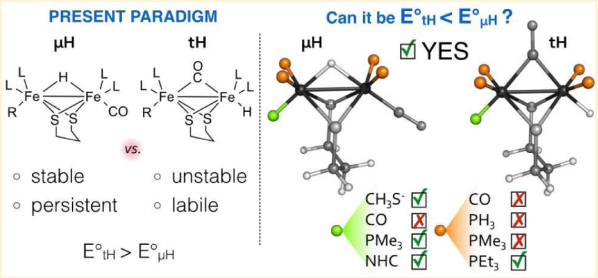

INTRODUCTION

Production of molecular hydrogen (H_2) has become a target of primary importance in the last years because of its nature as a clean, high-energy-density, and renewable energy carrier.[1] More and more restrictive measures against anthropogenic carbon dioxide (CO_2) emissions have led to a switch from a "fossil fuel economy" toward a "hydrogen economy", one of most cogent issues that the world community has to deal with in the next years. In this perspective, [FeFe]-H_2ase, a class of enzymes able to efficiently catalyze the reversible formation of H_2 starting from protons and electrons, has drawn increasing interest by a variegated scientific community.[2,3] These enzymes, which contain a $[Fe_6S_6]$ moiety (referred to as the H-cluster), are characterized by a high rate of H_2 evolving reaction (HER), but they are very active also in the opposite way.[2] The H-cluster contains a canonical cubane cluster, $[Fe_4S_4]$, linked through a cysteinyl sulfur group to a Fe_2 subunit, where both H_2 production and oxidation take place. The two Fe ions, referred to as proximal (Fe_p) or distal (Fe_d) with respect to the cysteine residue, are coordinated by CO and CN^- ligands and chelated by $(SCH_2)_2X$ (X = NH, adt).[4−8] The two cyanides are anchored to the protein, one through the backbone and the other via a lysine conserved in all [FeFe]-H_2ases.[9−11]

The unique structure of the [FeFe]-H_2ase active site encouraged the research of novel bioinspired complexes, in order to better figure out structure−activity relationships and ultimately design new synthetic catalysts. The reduction of protons, once these have bound the cofactor in its Fe^IFe^I redox state, is a key step in HER both in enzyme catalysis and in that performed by synthetic analogues. Therefore, the present study is specifically focused on the first reduction occurring during catalytic HER: $[Fe^{II}Fe^{II}]$-H + $e^- \rightarrow [Fe^IFe^{II}]$-H, with the H coordination mode being unspecified. The importance of mixed-valence $[Fe^IFe^{II}]$-H species resides in their likely intermediacy in both the enzyme turnover and also electrocatalysis performed by synthetic $(Fe^I)_2$ analogues.[12,13]

It has been postulated that in the enzyme the proton binds in a terminal fashion on the vacant apical position of Fe_d,[14−16] even though t-H has been reported to be thermodynamically less stable than the corresponding FeFe μ-H.[10] Thus, it is

Received: July 6, 2015
Published: September 11, 2015

DOI: 10.1021/acs.inorgchem.5b01495
Inorg. Chem. 2015, 54, 9529−9542

conceivable that a mechanism of rearrangement could, in principle, turn the t-H isomer into the μ-H isomer. However, two $Fe_2(CN)_2$–enzyme (aforementioned) interactions are expected to hinder the isomerization at Fe_d, preventing the formation of a less reactive μ-hydride. The importance of the key lysine anchoring one cyanide in *Clostridium pasteurianum* [FeFe]-H_2ase is such that its replacement results in a complete loss of activity because of the missed fixing of the H-cluster to the enzyme active site.[17] Despite the biological relevance of t-Hs, their experimental detection in synthetic analogues has been rare, and it even requires special conditions because of their spontaneous tendency to isomerize to μ-Hs, as is generally and widely reported (vide infra for more specific cases).[18] An intimate mechanism of rearrangement from t-H to μ-H in some bioinspired compounds has been proposed in a density functional theory (DFT) computational investigation illustrating the energetic viability of the process.[19] Such viability has been predicted to be absent in the enzyme cofactor, in a recent work by Reiher's group.[20] These data reinforce the aforementioned idea that (too) stable bridging hydrides would form a thermodynamic sink also in the enzyme if a kinetic device was not present to freeze the t-H-to-μ-H isomerization. Terminal (or "single Fe") coordination of hydrides in synthetic mimics of the enzyme was first detected by Ezzaher et al. in solution at low temperature.[21] In these conditions, the isomerization process leading to bridging isomers is certainly slow to occur. In the same study, it was shown that protonation of the asymmetric complex $[Fe_2(pdt)(CO)_4(dppe)]$ [dppe = 1,2-$C_2H_2(PPh_2)_2$] at two different temperatures (−50 and −75 °C) led to the formation of two different t-Hs, on the $(CO)_3$ Fe atom or on the (CO)(dppe) Fe atom, respectively.[21] The first solid-state (X-ray diffraction) characterization of a terminal hydride of a diferrous complex was performed by the Rauchfuss' group.[22] t-Hs were also characterized spectroscopically for a family of complexes with bulky bis-phosphine ligands [dppv = 1,2-*cis*-$C_2H_2(PPh_2)_2$].[23,24] In one of these studies, the persistence of the terminal isomer was such to allow its redox potential measurement, along with that of μ-H. Analysis on pdt and adt derivatives of species investigated in the same study showed that t-Hs reduce at potentials of 100–200 mV less negative than their bridging counterparts ($\Delta E^\circ_{\text{t-H}-\mu\text{-H}} > 0$).[22] As observed by Pickett's group, the reduction potential gap could be correlated with the spin density distribution derived from DFT analysis: while in μ-H, the spin density is delocalized on both Fe atoms,[25] in t-H, it is localized on the Fe atom with no hydride. Finally, Zaffaroni et al. reported that the protonation of $[Fe_2(adt)(CO)_2(PMe_3)_4]$ yields only t-H as a result.[26]

Aimed at working out the issue "stable/less reactive μ-H vs unstable/reactive t-H", one strategy has been adopted to date: the search for stable t-Hs, or at least able to persist in solution long enough to be reduced (and protonated again). The use of bulky electron-donor ligands of the Fe_2 core has allowed Rauchfuss' group to obtain a derivative functioning in this last sense. Nonetheless, also because of the aforementioned ever-growing interest toward H_2ases,[4,18,27] it may be worth exploring new strategies. Along this way, it can be remarked that a hydride in the bridging position between Ni and Fe atoms has been unequivocally identified by different spectroscopy techniques in [NiFe]-H_2ase, and it has been demonstrated that it is a catalytically active intermediate.[28] Even outside the H_2ase family, other outstanding examples of bioorganometallic clusters forming μ-hydrides are known, such as FeMo-co embedded in the nitrogenase active site.[29] This would suggest that, in nature, there is no intrinsic disadvantage for catalytic processes to pass through metal–metal bridging hydride forms.

Thus, we have searched for the combination of ligands that afforded species with $\Delta E^\circ_{\text{t-H}-\mu\text{-H}} < 0$, thus indicating a higher (or at least as high as) redox reactivity of μ-H versus t-H. This would allow us to overturn the paradigm, valid certainly in the [FeFe]-H_2ase modeling, that depicts μ-H as persistent-less reactive, whereas t-H is labile-reactive. Herein, by the term "reactive", we are meaning "provided with higher (less negative compared to other redox references) reduction potential". DFT results show that pushing simultaneously on both the basicity and bulk of diiron ligands affords a μ-H with a reduction potential more favorable than that of t-H. The electron richness of the Fe_2 core has been revealed to affect $\Delta E^\circ_{\text{t-H}-\mu\text{-H}}$, but the factor proven to be crucial in turning the sign of the redox gap in favor of t-H is the steric repulsion introduced by means of bulky tertiary phosphines. Because t-H and μ-H feature different bond patterns inside their molecular structure, they behave differently upon reduction, and this unravels the origin of the correlation that emerged between $\Delta E^\circ_{\text{t-H}-\mu\text{-H}}$ and the ligand number/type.

COMPUTATIONAL METHODS

All DFT calculations have been carried out with the *TURBOMOLE* suite of programs,[30] applying the resolution of identity technique,[31] using the all-electron TZVP basis set[32] and the BP86 pure functional.[33,34] This level of theory has been shown to be suitable and reliable for the investigation of [Fe–Fe]-H_2ase models.[10,35−38] Especially when dealing with computing redox potentials of diiron dithiolates mimicking H_2ases, the choice of BP86 versus B3LYP[34,39,40] proved to be the most reliable.[41]

Aiming at computing theoretical values of standard reduction potentials (E°) that best reproduced those experimentally observed, we initially adopted a protocol based on the Born–Haber cycle.[41,42] Free-energy changes associated with the half-reactions are shown in Scheme 1.

Scheme 1. Born–Haber Cycle Used for the DFT Evaluation of Redox Potentials

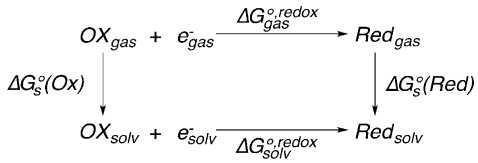

The standard Gibbs free energy is calculated as follows:

$$\Delta G^{\circ,\text{redox}}_{\text{solv}} = \Delta G^{\circ,\text{redox}}_{\text{g}} + \Delta G^{\circ}_{\text{s}}(\text{Red}) - \Delta G^{\circ}_{\text{s}}(\text{Ox}) \quad (1)$$

The standard one-electron redox potential E° is calculated by eq 2:

$$\Delta G^{\circ,\text{redox}}_{\text{solv}} = -FE^\circ \quad (2)$$

where ΔG is calculated as in eq 1 and F is the Faraday constant, 23.061 kcal mol^{-1} V^{-1}. In order to include entropy, zero-point-energy (ZPE), and enthalpy contributions into the self-consistent-field (SCF) energy (E_{SCF}), three different contributions ($q_{\text{translational}}$, $q_{\text{rotational}}$, and $q_{\text{vibrational}}$) have been considered to evaluate the molecular partition function.[43] The T and P values were generally set at 298.15 K and 1 bar, respectively (other T values have been used in specific cases in which the experimental conditions were explicitly different). Because of the high values of the SCF wavenumbers arising from the harmonic approximation, a scaling factor of 0.9914 was applied.[30] The solvent (CH_2Cl_2) polarizing effect has been modeled according to the COSMO approach,[44,45] by considering a polarizable continuum medium characterized by ε = 9.01. Because the experimental value is

DOI: 10.1021/acs.inorgchem.5b01495
Inorg. Chem. 2015, 54, 9529–9542

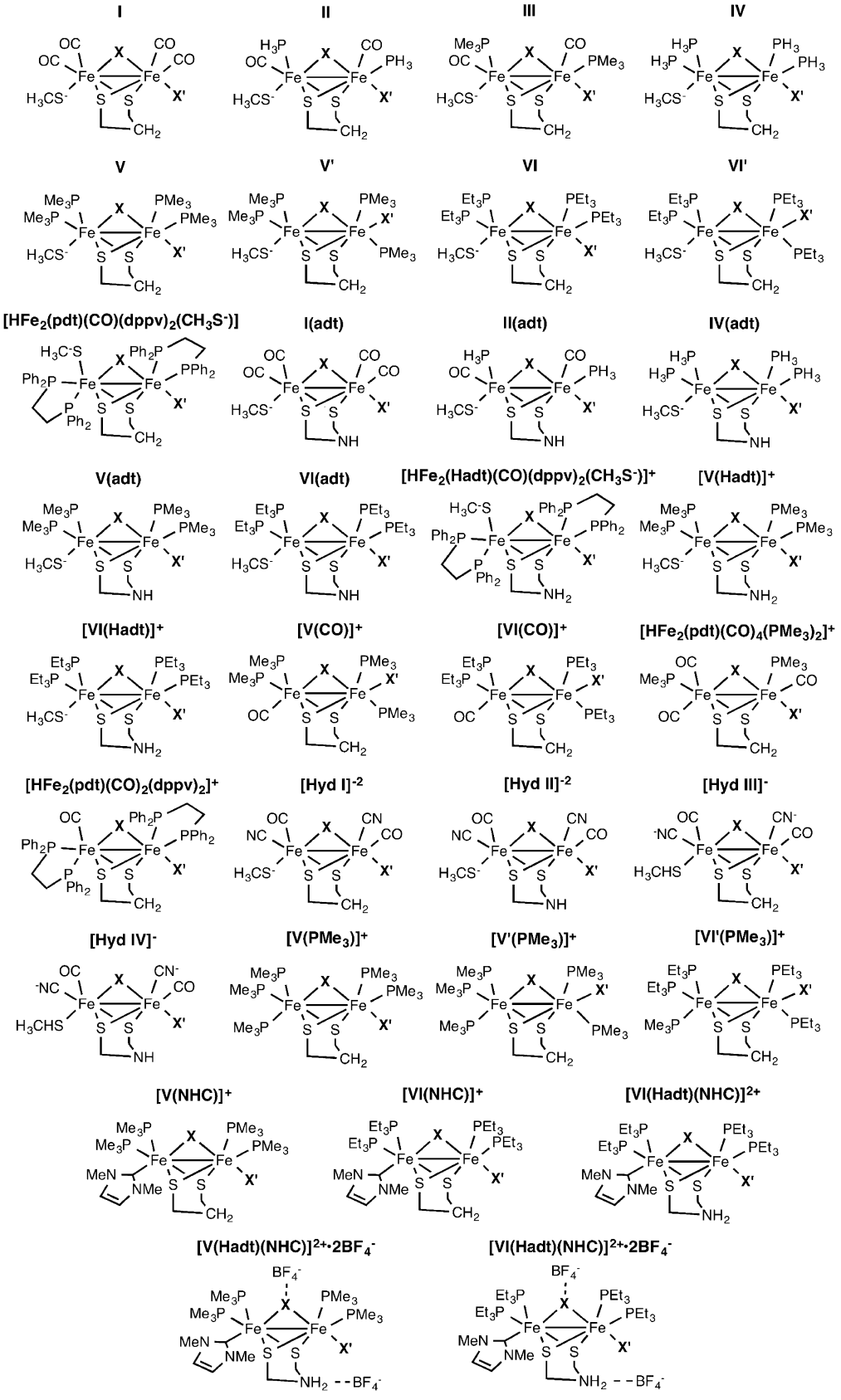

Figure 1. Full set of models investigated in the present study. In μ-H isomers, X = H^- and X′ = CO, whereas in t-H isomers, X = CO and X′ = H^-. [**Hyd I**]$^{2-}$ = $[HFe_2(pdt)(CO)_3(CN)_2(SCH_3)]^{2-}$, [**Hyd II**]$^{2-}$ = $[HFe_2(adt)(CO)_3(CN)_2(SCH_3)]^{2-}$, [**Hyd III**]$^-$ = $[HFe_2(pdt)(CO)_3(CN)_2(SCH_3)]^-$, and [**Hyd IV**]$^-$ = $[HFe_2(adt)(CO)_3(CN^-)_2(SCH_3)]^-$. Only the lowest-energy stereoisomer [related to possible different rotamers at the $Fe_d(X)_3$ group] of each species is shown in the picture. In **V′**, **VI′**, [**V(CO)**]$^+$, [**VI(CO)**]$^+$, [**V′(PMe$_3$)**]$^+$, and [**VI′(PMe$_3$)**]$^+$ species, the correct t-H disposition is to be obtained by rotating the $Fe_d(X)_3$ group by 120°.

DOI: 10.1021/acs.inorgchem.5b01495
Inorg. Chem. 2015, 54, 9529−9542

known for the gap of the standard reduction potential ($\Delta E^{\circ}_{\text{t-H}-\mu\text{-H}}$) associated with the species $[HFe_2(pdt)(CO)_2(dppv)_2]^+$ (Figure 1),[23] we have tested which method provided the best match of theory versus experiment, among the following: ΔE (gas-phase condition), ΔE_{solv} (structure optimization in COSMO CH_2Cl_2), $\Delta E_{solv(SCF)}$ (gas-phase value + single-point COSMO corrections, CH_2Cl_2), ΔG (ΔE + thermal/entropic corrections), ΔG_{solv} (ΔE_{solv} + thermal/entropic corrections), and $\Delta G_{solv(SCF)}$ ($\Delta E_{solv(SCF)}$ + thermal/entropic corrections).

As aforementioned, $\Delta G_{solv(SCF)}$ represents in theory the formally correct approach because it includes entropic and thermal contributions and solvent effects as well. However, in the case under investigation, $\Delta E_{solv(SCF)}$ values afforded the closest match of theory versus experiment concerning $\Delta E^{\circ}_{\text{t-H}-\mu\text{-H}}$ (exp value, 200 mV;[23] computed value arising from $\Delta E_{solv(SCF)}$, 216 mV; value from ΔG_{solv}, 172 mV; see also Table S1 to compare the results obtained from other ΔE_X calculations). Besides reproducing $\Delta E^{\circ}_{\text{t-H}-\mu\text{-H}}$, our computational model allowed us to obtain a fine match (max error = 0.14 V) of theory versus experiment of redox potentials referenced to electrodes employed experimentally (such as Fc^+/Fc).[42] The better performance of ΔE versus ΔG in the present case is likely due to a cancelation error effect arising from approximations normally used to turn ΔE into ΔG (i.e., ideal gas approximation, separation into components of the total energy, harmonic approximation, etc.).

RESULTS AND DISCUSSION

The main aim of the present work is to investigate the possibility of designing bridging hydrides that show more favorable reduction potentials than terminally coordinated congeners and implicitly unveil which factors are more relevant in making one-electron reduction of t-H generally easier than that of bridging hydrides.[23,24] As aforementioned, the elementary event that we are interested in is the first reduction occurring during catalytic HER:

$$[Fe^{II}Fe^{II}]\text{-H} + e^- \rightarrow [Fe^{I}Fe^{II}]\text{-H} \quad (3)$$

with the H coordination mode being unspecified in eq 3. The mixed-valence $[Fe^{I}Fe^{II}]$-H reduction product has been postulated to be formed in the catalytic turnover of both the enzyme and its synthetic analogues.[12,13] The results have been divided into different sections for clarity. The first four sections, A, B, C, and D, are explicitly focused to investigate if and how different variations of the ligands of the Fe_2 core can affect $\Delta E^{\circ}_{\text{t-H}-\mu\text{-H}}$, pointing out those variants featuring negative $\Delta E^{\circ}_{\text{t-H}-\mu\text{-H}}$.

More specifically, in section A, the focus is on variations of all ligands (L) but the apical one at Fe_p and the xdt chelate. In section B, also because the methylthiolate ligand has never been employed in biomimetic compounds, we investigated the effect of its replacement with other ligands employed in inorganic synthesis, such as CO, PMe_3, and N-heterocyclic carbene (NHC), with the latter already proven to be a good donor, similarly to the biological cyanide ligand.[48] Section C explores the effects on/of protonating the apical CH_3S^-, whereas section D illustrates the effects of switching from pdt to adt (in both its neutral and N-protonated forms).

Section E does not deal with the main issue raised in the title of the present study but is aimed at extending the thermodynamic characterization (of HER) of a derivative that section A has shown to be of potential interest to the design of new [FeFe]-H_2ase models.

A. Analysis of the Effects on $\Delta E^{\circ}_{\text{t-H}-\mu\text{-H}}$ Induced by Variations of Fe_2 Ligands (Different from xdt and the Apical CH_3S^-). Because cyanides have been seldom used as iron ligands in the synthetic modeling of H_2ase, due to their undesired proton affinity,[27] carbonyls and different phosphines[46,47] have been used in the present study as ligands of the $Fe_2(SR)_2$ center. Starting from the atomic coordinates of the PDB structure (1HFE), canonical H-cluster ligands were modified to obtain series $[HFe_2(pdt)(PR_3)_n(CO)_{5-n}CH_3S]$ (n = 0, 2, 4; R = H, Me, Et; Figure 1). The whole set of complexes is shown in Figure 1, with X/X′ representing H and CO ligands switching relative positions in bridging versus terminal hydrides. Upon reduction, the $[2Fe]_H$ core of μ-H and t-H is formally reduced from $Fe^{II}Fe^{II}$ to $Fe^{II}Fe^{I}$. The reported values for $E^{\circ}_{\text{t-H}}$ and $E^{\circ}_{\mu\text{-H}}$ (V) and $\Delta E^{\circ}_{\text{t-H}-\mu\text{-H}}$ (mV) have been referenced to the absolute redox potential of the Fc^+/Fc couple, normally employed in electrochemical investigations related to [FeFe]-H_2ase.

Table 1 is related to the first subset of compounds considered, $[HFe_2(pdt)(PR_3)_n(CO)_{5-n}CH_3S]$: the aim was in this case to analyze the effect of systematically increasing the number (and type) of phosphines, evaluating the role of their size (steric bulk) in changing $\Delta E^{\circ}_{\text{t-H}-\mu\text{-H}}$. In addition, because the complexes in the model set contain an apical methylthiolate at Fe_p, this analysis has been done with the goal of modeling the role of the biogenic cysteine.

Table 1. Computed Redox Potentials (vs Fc^+/Fc) of μ-H and t-H for the Series $[HFe_2(pdt)(PR_3)_n(CO)_{5-n}CH_3S^-]$

compound	$E^{\circ}_{\mu\text{-H}}$ (V)	$E^{\circ}_{\text{t-H}}$ (V)	$\Delta E^{\circ}_{\text{t-H}-\mu\text{-H}}$ (mV)
I	−1.782	−1.589	193
II	−2.415	−2.230	185
III	−2.677	−2.478	199
IV	−2.990	−2.836	154
V	−3.451	−3.175	276
V′	−3.249	−3.175	74
VI	−3.185	−3.198	−13
VI′	−2.648	−3.198	−550

The results in Table 1 show that t-H is more easily reduced than μ-H, in all species considered (except **VI** and **VI′**, vide infra), which is generally in line with the experimental data related to the biomimetic models investigated to date.[23] As expected, increasing the electronic density on the [2Fe] core of the various species implies more negative E°.

Nonetheless, increasing the number of phosphines coordinated to the Fe_2 core does not appear to significantly affect the reduction potential gap, showing rather an irregular trend, on going from **I** to **V**, with the last one featuring the clearest preference for t-H reduction. Unexpectedly, replacing PMe_3 with PEt_3 (i.e., switching from **V** to **VI**) causes E° to become approximately equivalent in t-H versus μ-H ($\Delta E^{\circ}_{\text{t-H}-\mu\text{-H}}$ = −13 mV). Moreover, **VI** is also the only species showing a bridging form less stable than the terminal one, at both the $Fe^{II}Fe^{II}$-H (by 4.4 kcal mol^{-1}) and $Fe^{II}Fe^{I}$-H (by 4.1 kcal mol^{-1}) states. As for the **V′** and **VI′** μ-H species, they are isomers (with basal−apical disposition of PX_3 ligands at Fe_d) of **V** and **VI**, respectively. Reduction of these isomers has been investigated because they are very close in energy (within the DFT accuracy value) to the dibasal forms **V** and **VI**. Thus, both **V** and **VI** should be considered as two-component systems, denoted as **V**/**V′** and **VI**/**VI′**, given a likely coexistence of both isomers in solution.

Like **VI**, also **VI′** features a t-H more stable than μ-H by more than 2 kcal mol^{-1} at the $Fe^{II}Fe^{II}$-H state, whereas **V**/**V′** shows a preference for μ-H (rather limited in the case of **V′**).

DOI: 10.1021/acs.inorgchem.5b01495
Inorg. Chem. 2015, 54, 9529−9542

Table 2. [Fe−Fe] and Other Selected Distances (Å) in the t-H and μ-H Isomers in the I−VI Set

	μ-H						t-H					
	$Fe^{II}Fe^{II}$			$Fe^{II}Fe^{I}$			$Fe^{II}Fe^{II}$			$Fe^{II}Fe^{I}$		
compound	Fe−Fe	Fe_p−H	Fe_d−H	Fe−Fe	Fe_p−H	Fe_d−H	Fe−Fe	Fe_p−C(O)	Fe_d−C(O)	Fe−Fe	Fe_p−C(O)	Fe_d−C(O)
I	2.600	1.644	1.721	2.779	1.593	1.854	2.526	2.000	1.978	2.704	1.990	1.998
II	2.598	1.641	1.739	2.690	1.626	1.765	2.505	1.976	1.953	2.661	1.960	1.973
III	2.615	1.640	1.750	2.799	1.589	1.893	2.501	1.978	1.938	2.664	1.961	1.966
IV	2.592	1.689	1.789	2.678	1.655	1.844	2.487	1.992	1.922	2.618	1.941	1.965
V	2.719	1.689	1.790	2.831	1.656	1.844	2.541	1.992	1.922	2.672	1.941	1.965
VI	2.837	1.751	1.823	3.419	1.545	2.963	2.573	1.995	1.931	2.723	1.943	1.978

This result is serendipitous, although particularly relevant, because stabilization of terminal versus bridging hydrides has been and still is to be considered a challenge from a synthetic standpoint.

Inspection of all of the reduced μ-H structures reveals that only **VI** features one Fe−H bond that is completely cleaved, to such an extent that H^- coordination becomes terminal (specifically, at Fe_p, data are not shown). In light of the reported higher reactivity toward protons of t-H form[22] and because a second protonation is a requisite for the HER occurrence, the characteristics identified in **VI** could unravel interesting perspectives.

In particular, because $\Delta E^\circ_{\text{t-H}-\mu\text{-H}}$ associated with **VI** is near zero, whereas it is clearly >0 for the very similar **V**, a proper tailoring of the second coordination sphere of Fe could allow one to tune such redox parameters. Curiously, however, the narrowing (and the sign inversion) of $\Delta E^\circ_{\text{t-H}-\mu\text{-H}}$ in **VI** is concomitant with the presence of a more stable t-H than μ-H so as to indicate the "classical" strategy and that pursued herein could be related.

Aimed to test the robustness of our findings for **V** versus **VI**, an extensive torsional sampling has been performed within the phase space of the Et groups linked to P atoms. This means that calculations have been carried out several times by starting from different initial spatial orientations of the 12 Et groups. The results show that the three-dimensional arrangement of Et groups originally found in **VI** and **VI′** μ-H isomers actually corresponds to the most stable. As aforementioned, **V** and **VI** differ only by the Me versus Et nature of R_3P, but the $\Delta E^\circ_{\text{t-H}-\mu\text{-H}}$ variation on going from one to the other is the most evident of the whole subset shown in Table 1. It could be argued that PMe_3 and PEt_3 have so similar basic properties that the discrepancy that emerged between **V** and **VI** should be ascribed to steric repulsions possibly induced by the different bulk of R groups. Moreover, a rationale is to be found for the irregular trend observed for $\Delta E^\circ_{\text{t-H}-\mu\text{-H}}$ in Table 1: on going from electron-poorer to electron-richer compounds, the number/type of P ligands does not clearly affect the E° gap, whose sign, yet, is even reverted in the presence of bulky Et groups on 4-P species. This would suggest that, upon creation of the conditions whereby steric effects can play a role (for example, in a highly substituted diiron core), they have an evident impact. The nonlinear trend outlined in Table 1 for $\Delta E^\circ_{\text{t-H}-\mu\text{-H}}$ shows that sign inversion occurs in an unpredictable way. This supports the following precedent statement: the number of σ-donors on the diiron derivative is not intrinsically a determinant factor, but it becomes, however, a crucial prerequisite insofar as it allows some peculiar effects to unveil their role on $\Delta E^\circ_{\text{t-H}-\mu\text{-H}}$ variation.

Even more surprisingly, not only the number of σ-donors but also the donor strength is not per se sufficient to rationalize the observed picture. In fact, Tolman, Pickett, and Lever parameters[49−52] suggest that the PEt_3 group is a stronger donor ligand than PMe_3 is, even though other properties such as the pK_a's of PMe_3 and PEt_3 are quite similar (8.65 for PMe_3 vs 8.69 for PEt_3).[53] Yet, as reported in Table 1, $E^\circ_{\mu\text{-H}}$ of **V** is more negative than $E^\circ_{\mu\text{-H}}$ of **VI** and **VI′**, whereas the reversal is observed in t-H congeners of the same species. All such "apparent" anomalies must therefore be explained, invoking steric factors. The last statement is even reinforced considering that Fe-PEt_3 (2.392 Å, avg) bond distances are generally longer than those of Fe-PMe_3 (2.327 Å, avg). This is another counterintuitive observation with respect to the outcome that we had figured out based on the stronger donor properties of PEt_3 versus PMe_3.[50−52]

To corroborate our hypothesis and to pinpoint the intimate reason underlying the **V** versus **VI** reductive behavior, a series of structural parameters have been analyzed in the **I**−**VI** set. **V′** and **VI′** have been excluded from such kinds of analyses for reasons that will became clear subsequently. Analysis of the data in Table 2 will be crucial to evaluating if and how a given structure is affected by intramolecular repulsive strain; that is the factor that we will show to be decisive to explain our results on $\Delta E^\circ_{\text{t-H}-\mu\text{-H}}$.

Table 2 shows a series of interatomic distances aimed at monitoring structural variations upon reduction in the molecular region containing the Fe(X)−Fe(X′) moiety, throughout the **I**−**VI** set. This allows us to gain information on (i) the actual strength of the Fe−Fe interaction and (ii) the symmetry degree of the hydride coordination to iron (terminal vs bridging character), upon going from $Fe^{II}Fe^{II}$ to $Fe^{II}Fe^{I}$ states.

It turns out to be evident that **VI** has a peculiar feature in the whole set: upon reduction, its μ-H undergoes a complete breaking of the Fe−Fe bond with concomitant generation of relatively separated Fe subunits, the first containing a five-coordinated Fe_d and the second including a six-coordinated Fe_p. The last one is coordinated by hydride in a completely terminal fashion. The high similar (to **VI**) compound **V** does not behave analogously, once reduced. Indeed, **V** ($Fe^{II}Fe^{I}$) displays elongation of both Fe−Fe and Fe_d−H distances, but quantitatively compared to those observed in **VI**, these are definitely moderate. Such a different behavior in so similar derivatives occurring for only one of the two isomeric forms could help to explain the drop of $\Delta E^\circ_{\text{t-H}-\mu\text{-H}}$ observed in Me_3P versus Et_3P species. Otherwise stated, the cause of the structural differences for **V** versus **VI** in their reduced state could be at the ground of the sign inversion of $\Delta E^\circ_{\text{t-H}-\mu\text{-H}}$. We propose that intramolecular steric repulsions are introduced by enlarging the R size of phosphine ligands upon going from **V** to **VI**. This produces a strain (or destabilization) in the $Fe^{II}Fe^{II}$ state of **VI**, which is unique in the **I**−**VI** sets of compounds. This

DOI: 10.1021/acs.inorgchem.5b01495
Inorg. Chem. 2015, 54, 9529−9542

destabilization affects both μ-H and t-H of **VI**, but reduction can alleviate repulsive interactions (either by mutually separating the two Fe subunits or by another way, vide infra) only in the bridging isomer but not in t-H, as emerged from a comparison of the structural parameters of **V** versus **VI**.

Thus, it becomes of primary importance to understand why reduction can separate the two Fe subunits of μ-H but not those of t-H in the case of **VI**. Some features being present exclusively in t-H may prevent the strain from being relaxed upon reduction. Indeed, all terminal-bound hydrides have a CO in the bridging position between the two Fe ions. Furthermore, the Fe−Fe-bridging CO is trans-oriented simultaneously to two strong electron donors (H^- and CH_3S^-): it is therefore predictable that, specifically in electron-rich derivatives, CO receives a large amount of electron density through a double π-back-donation from both Fe atoms. This implies the presence of two strong Fe−C(O)−Fe bonds (each with partial double-bond character), which can prevent dissociation of the two Fe subunits upon reduction. Bridging hydrides cannot show similar behavior because of the absence of π-acceptor properties by the H ligand. This results in μ-hydrido isomers of species affected by intramolecular destabilization (exactly as **VI**) being free to alleviate the strain thanks to reduction.

The observation of key distances associated with **V** (Table 2) brings to light that this derivative must not be affected by intramolecular strain, which implies that its reductive behavior should not deviate significantly from the other less substituted derivatives of Table 1. This indirectly indicates that, without steric factors influencing selectively the two hydrido forms of a given species, the observation of a more favorable redox potential associated with t-H must be governed by pure electronic factors.

As aforementioned, the DFT isomer speciation showed (limited to **V** and **VI** in their oxidized state) that the two possible ligand dispositions at Fe_d ($P_{dibasal}$ and $P_{apical-basal}$) are so close in energy that DFT accuracy does not allow an unequivocal resolution of their relative stability. Therefore, the two stereoisomers should be fairly predicted to coexist in a thermodynamically equilibrated solution. Redox potentials have therefore been calculated also for **V′** and **VI′**. Interestingly, reduction causes this time the loss of the apical PX_3 from Fe_d coordination in the sole instance of **VI′**, while $\mathbf{V'}_{Fe^{II}Fe^{I}}$ was still a bis-six-coordinated Fe species. The Fe−PEt_3 bond breaking upon reduction leads to a larger release of molecular strain compared to that observed for reduction of the dibasal isomer, as demonstrated by Table 1 data (comparing **VI** vs **VI′** $\Delta E^{\circ}_{\text{t-H}-\mu\text{-H}}$). Thus, dissociating a P ligand from Fe represents the other way (hinted previously) that μ-Hs of strained/unstable species have for relaxing accumulated repulsions. Of course, because **VI** and **VI′** share the same t-H structure, the rationale that justifies why the strain release occurs only in μ-Hs is the same as that outlined previously. These results support quite incontrovertibly the idea that a proper modulation of the intramolecular sterics can influence the $\Delta E^{\circ}_{\text{t-H}-\mu\text{-H}}$ gap.

Frontier molecular orbital (FMO) analysis has been then performed to pinpoint which electronic properties are mostly influenced by the structural difference in **V** versus **VI**. From inspection of the singly occupied molecular orbital (SOMO) in reduced states of **V** versus **VI**, shown in Figure 2, it is evident that the molecular strain affecting **VI** and (but not **V**) finds release upon reduction in μ-H, whereas in t-H, there is actually a strain retention. A comparison of E_{SOMO} values shows that there is complete consistence with the more favorable

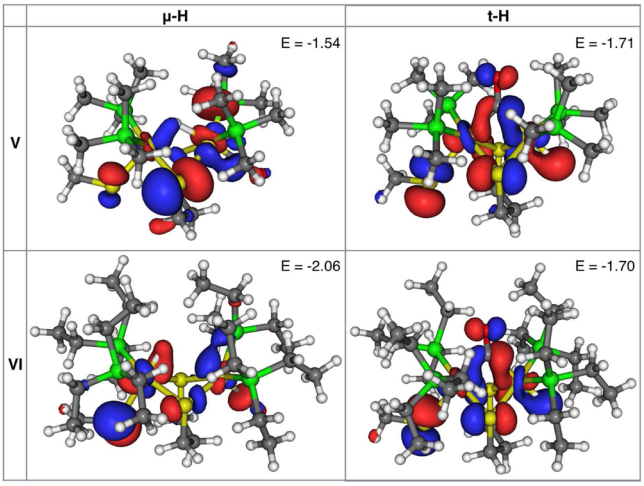

Figure 2. E_{SOMO} (eV) and electronic distribution in reduced states of both t-H and μ-H for derivatives **V** and **VI**. The isosurface cutoff value is 0.03 atomic units.

reduction of t-H versus μ-H in **V** ($\Delta E^{\circ}_{\text{t-H}-\mu\text{-H}} > 0$; Table 1) and simultaneously with the reverse behavior in **VI** ($\Delta E^{\circ}_{\text{t-H}-\mu\text{-H}} < 0$). Also some differences are detectable in the atomic orbital composition (with consequential unequal distribution) of the two SOMOs in μ-hydrides of **V** versus **VI**, whereas such a parameter is practically unchanged when looking at the SOMO of t-Hs of the same species. Besides **V** and **VI**, other compounds have been investigated by FMO analysis, and the results are reported in Table S5. Finally, spin-density analysis regarding $Fe^{II}Fe^{I}$ species has been performed: the results are shown in the Supporting Information because they are not relevant for the current discussion.

In Scheme 2, all results presented and discussed in section A are summarized.

B. Effect of the Replacement of the Apical CH_3S^- with CO/PMe_3/NHC in V (4-PMe_3) and VI (4-PEt_3). Heretofore, we have considered complexes featuring the CH_3S^- ligand, a mimic of the cysteinyl sulfur bridge that links the Fe_4S_4 cluster to the Fe_2S_2 center.[4−7] Nonetheless, we already mentioned that CH_3S^- is not normally employed in the synthetic chemistry of H_2ases.[54] Thus, we set out to investigate the effect of replacing it with other ligands more routinely used synthetically, such as neutrally charged CO, PMe_3, and also NHC.

The results showing E°, $\Delta E^{\circ}_{\text{t-H}-\mu\text{-H}}$, and all of those structural parameters that are useful to evaluating the strain release upon reduction of the various species are reported in Tables 3 and 4.

First, it is evident that the **V**-like versus **VI**-like comparison confirms the essential role of intramolecular repulsions and their release upon reduction for justifying the $\Delta E^{\circ}_{\text{t-H}-\mu\text{-H}}$ variation. The presence of the CO group in place of the methylthiol group makes $\Delta E^{\circ}_{\text{t-H}-\mu\text{-H}}$ significantly positive, indicative of μ-H reduction clearly disfavored versus t-H reduction. The importance of the simultaneous presence of two σ-donors trans-oriented to bridging CO in terminal hydrides has already been invoked as the reason that prevents strained t-H (of the **VI**/**VI′** system) from being energy-relaxed. Therefore, $[\mathbf{VI(CO)}]^+$-t-H can relax, as well as μ-H, thus not showing that different behavior upon reduction of t-H versus μ-H, which is necessary to observe $\Delta E^{\circ}_{\text{t-H}-\mu\text{-H}}$ inversion. Indeed, the true reason for which the oxidized $[\mathbf{VI(CO)}]^+$-t-H is strained, despite the presence of two acceptors (with the CO

DOI: 10.1021/acs.inorgchem.5b01495
Inorg. Chem. 2015, 54, 9529−9542

Scheme 2. Effects of L Variations on $\Delta E^{\circ}_{\text{t-H}-\mu\text{-H}}$ (Also Designated as ΔE° for Simplicity) and Results Rationalization

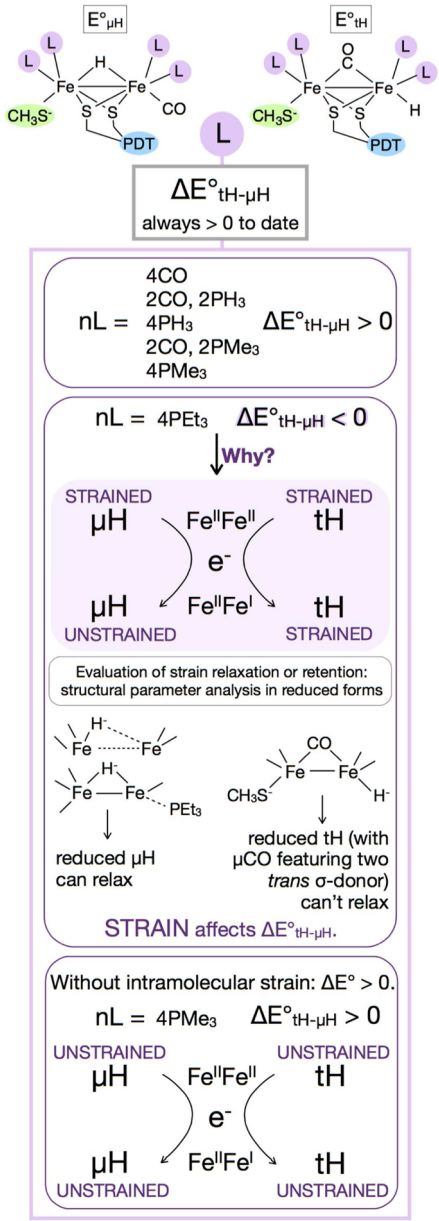

replacing CH_3S^- and μ-CO), whereas, for example, $[\mathbf{VI'(PMe_3)}]^+$ is not strained is rather subtle and is more complicated than depicted here. It requires invoking electronic effects, which have been discussed in the following, after presentation of the concepts illustrated in Figures 3 and 4.

We expected that substitution of CH_3S^- by PMe_3 ($[\mathbf{VI'(PMe_3)}]^+$) would lead to outcomes analogous to those of **VI**/**VI′**. These findings can be explained by the σ-donor nature of Me_3P, which, although less strong compared to the thiolate, is well-known. In this peculiar case, we have studied only one stereoisomer at Fe_d because the other is very unstable (data not shown). $[\mathbf{VI'(PMe_3)}]^+$ actually shows strongly negative $\Delta E^{\circ}_{\text{t-H}-\mu\text{-H}}$ (Table 3), but the reason underlying this result requires application of the "strain release" model in a slightly different way. Because the apical PMe_3 is a weaker donor than thiolate, it cannot trigger the formation of a Fe_p–

Table 3. Computed Standard Redox Potentials (E° vs Fc^+/Fc) and $\Delta E^{\circ}_{\text{t-H}-\mu\text{-H}}$ of $[HFe_2(pdt)(PX_3)_4(CO)Y]$ (X = Me in V/V′ and X = Et in VI/VI′; Y = CO, PMe_3, and NHC)[a]

complex	$E^{\circ}_{\mu\text{-H}}$ (V)	$E^{\circ}_{\text{t-H}}$ (V)	$\Delta E^{\circ}_{\text{t-H}-\mu\text{-H}}$ (mV)
V	*−3.451*	*−3.175*	*276*
V′	*−3.249*	*−3.175*	*74*
VI	*−3.185*	*−3.198*	*−13*
VI′	*−2.648*	*−3.198*	*−550*
$[\mathbf{V(CO)}]^+$	−2.201	−2.022	179
$[\mathbf{VI(CO)}]^{+*}$	−2.649	−1.944	705
$[\mathbf{V(PMe_3)}]^+$	−2.645	−2.353	292
$[\mathbf{V'(PMe_3)}]^+$	−2.647	−2.353	114
$[\mathbf{VI'(PMe_3)}]^{+*}$	−1.476	−2.042	−566
$[\mathbf{V(NHC)}]^+$	−2.840	−2.626	214
$[\mathbf{VI(NHC)}]^+$	−2.523	−2.568	−45

[a]In complexes designated with an asterisk, the reduced form of μ-H loses an apical phosphine, originally trans-oriented to hydride, whereas $[\mathbf{VI(NHC)}]^+$ is the only 4-PEt_3 system in which the strain release occurs through breaking of Fe–Fe and one Fe–H bonds. Data shown in italics (already reported in Table 1) have been inserted as reference. As a reminder, the **V**/**V′** formula is $[HFe_2(pdt)(PMe_3)_4(CO)CH_3S]$, while the **VI**/**VI′** formula is $[HFe_2(pdt)(PEt_3)_4(CO)CH_3S]$. **V**/**VI** and **V′**/**VI′** differ for the phosphine disposition at Fe_d, as follows: **V** and **VI** feature a dibasal disposition, while **V′** and **VI′** feature an apical–basal disposition.

CO bond (2.921 Å) as strong as in the case of CH_3S^--based species **VI**/**VI′** (1.995 Å), essential for preventing relaxation of molecular strain in terminal hydrides. This entails that t-H of $[\mathbf{VI'(PMe_3)}]^+$ is not strained at all *already at the oxidized level* (i.e., before reduction; see Figure 3), as is clearly evidenced from the structural parameter analysis presented in Table 4. $\Delta E^{\circ}_{\text{t-H}-\mu\text{-H}}$ values and structural parameters associated with $[\mathbf{VI(NHC)}]^+$ qualitatively confirm all results observed for $[\mathbf{VI'(PMe_3)}]^+$. The quantitative difference ($\Delta E^{\circ}_{\text{t-H}-\mu\text{-H}}$ of the PMe_3 species is clearly more negative than that in the NHC one) is explained by the fact that the $[\mathbf{VI'(PMe_3)}]^+$ μ-H loses a phosphine upon reduction, while the $[\mathbf{VI(NHC)}]^+$ μ-H displays Fe–Fe and Fe–H bond breaking. This last reductive behavior has less impact on the E° gap (see also **VI** vs **VI′**) from a quantitative standpoint.

It may be argued at this point that also $[\mathbf{VI'(CO)}]^+$ should feature a $Fe^{II}Fe^{II}$ t-H repulsively unstrained, just like $[\mathbf{VI'(PMe_3)}]^+$ and $[\mathbf{VI(NHC)}]^+$. The apical CO is actually expected to induce an even weaker Fe_p–μ-CO bond trans to it, compared to those characterizing $[\mathbf{VI'(PMe_3)}]^+$ and $[\mathbf{VI(NHC)}]^+$. As can be viewed in Table 4 (for example, focusing on the Fe–Fe bond), $[\mathbf{VI'(CO)}]^+$ features structural parameters that are indicative of a strained oxidized state, at least more than the corresponding state in $[\mathbf{VI'(PMe_3)}]^+$ and $[\mathbf{VI(NHC)}]^+$. That is due to a couple of factors, the first being the fact that the most stable rotameric disposition of $[\mathbf{VI'(CO)}]^+$ at Fe_p is not $(CO)_{ap}$–Fe–$(PEt_3)_{2ba-ba}$ but instead $(PEt_3)_{ap}$–Fe–$(CO)_{ba}(PEt_3)_{ba}$. Such a result is probably due to the same aforementioned reason: two mutually trans-oriented CO's are less stable than that in a P–Fe–(CO) disposition. Thus, oxidized t-H-$[\mathbf{VI'(CO)}]^+$ has actually a donor (P) ligand in the apical position at Fe_p, just like $[\mathbf{VI'(PMe_3)}]^+$ and $[\mathbf{VI(NHC)}]^+$, so that the issue of the different strain (in the former vs the two latter species) remains unclear, unless electronic factors are invoked. To shed light on that, one has to consider that t-H-$[\mathbf{VI'(CO)}]^+$ has a less electron-rich Fe_2 core than that of the other two species because of the presence of

DOI: 10.1021/acs.inorgchem.5b01495
Inorg. Chem. 2015, 54, 9529–9542

Table 4. Fe_p-Fe_d and Fe_d-H Distances (Å) in Species of Table 3[a]

	μ-H				t-H			
	$Fe^{II}Fe^{II}$		$Fe^{II}Fe^{I}$		$Fe^{II}Fe^{II}$		$Fe^{II}Fe^{I}$	
compound	Fe_p-Fe_d	Fe_d-H	Fe_p-Fe_d	Fe_d-H	Fe_p-Fe_d	$Fe_p-CO(C)$	Fe_p-Fe_d	$Fe_p-CO(C)$
$[\mathbf{V(CO)}]^+$	2.648	1.662	2.792	1.680	2.641	2.526	3.093	2.999
$[\mathbf{VI(CO)}]^{+*}$	2.689	1.675	2.692	1.695	2.674	2.513	3.179	2.989
$[\mathbf{V(PMe_3)}]^+$	2.765	1.748	2.932	1.776	2.772	2.747	3.268	3.276
$[\mathbf{V'(PMe_3)}]^+$	2.718	1.702	2.885	1.802				
$[\mathbf{VI'(PMe_3)}]^{+*}$	2.779	1.710	2.719	1.721	2.920	2.921	3.379	3.297
$[\mathbf{V(NHC)}]^+$	2.711	1.702	2.873	1.846	2.768	2.679	3.214	3.144
$[\mathbf{VI(NHC)}]^+$	2.881	1.790	3.527	3.011	2.875	2.771	3.329	3.181

[a]In complexes designated with an asterisk, reduced μ-H loses an apical phospine trans-oriented to hydride, whereas $[\mathbf{VI(NHC)}]^+$ is the only 4-PEt_3 system in which the strain release occurs through breaking of Fe−Fe and one Fe−H bonds.

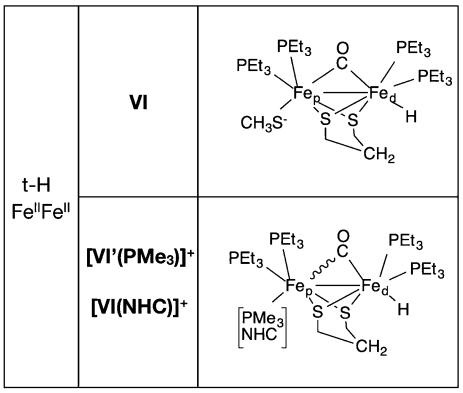

Figure 3. Neutrally charged apical donors implying a weakening of the Fe_p-CO bond in the cationic diferrous state of t-H: this causes $[\mathbf{VI'(PMe_3)}]^+$ and $[\mathbf{VI(NHC)}]^+$ to be unstrained structures, unlike **VI** (bearing apical CH_3S^-).

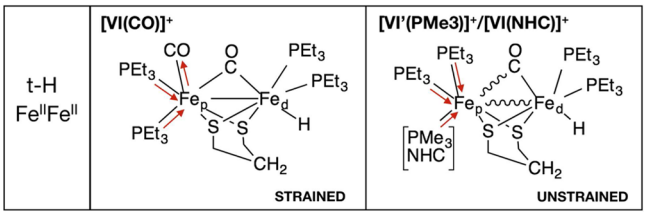

Figure 4. Schematic illustration of electronic factors underlying the presence of strain in t-H-$[\mathbf{VI'(CO)}]^+$ and the absence of strain in t-H-$[\mathbf{VI'(PMe_3)}]^+$ and t-H-$[\mathbf{VI(NHC)}]^+$.

CO versus NHC and PMe_3. This means that in t-H-$[\mathbf{VI'(CO)}]^+$ more electron density is drawn from the Fe_2 core compared to t-H-$[\mathbf{VI'(PMe_3)}]^+$ and t-H-$[\mathbf{VI(NHC)}]^+$ (see Figure 4). Although the 18-electron rule formally requires the presence of the Fe−Fe bond in the investigated species, it is yet conceivable that, in very electron-rich Fe_2 cores such as those in t-H-$[\mathbf{VI'(PMe_3)}]^+$ and t-H-$[\mathbf{VI(NHC)}]^+$, each Fe ion is already electronically saturated, so that the Fe−Fe formation is less mandatory than that in t-H-$[\mathbf{VI'(CO)}]^+$.

On a more general level, it can thus be confidently concluded that what ultimately determines the sign of $\Delta E^\circ_{\text{t-H}-\mu\text{-H}}$ is not necessarily the presence of factors keeping strained t-Hs from relaxing, whereas corresponding μ-Hs are able to do that (as illustrated in the **VI**/**VI'** case). Indeed, the crucial point is the different reductive behavior of t-H versus μ-H of a given species, in whatever fashion it may occur. It is relevant that the model we have devised to monitor the presence/absence of intramolecular strain remains valid in all of the instances we investigated, with the only variation residing in the manner of application of the model itself.

Identical behavior implies that t-Hs are reduced at potentials less negative than those of μ-Hs, whereas different behavior implies the opposite outcome. We stress that herein the "identical/different" couple refers to how/if the t-H versus μ-H of a particular instance changes its features in terms of the repulsive strain model that we set up and which could be coded as follows. Let "S" stand for "strained" and "US" for "unstrained molecule"; an identical reductive behavior t-H versus μ-H will be coded either by "S/S vs S/S" or by "US/US vs US/US" or finally by "S/US vs S/US". Any other combination of characters associated with the strain model will provide a "different" reductive behavior in the t-H/μ-H couple. This rationale can be schematically shown in Table 5, from which it is clear how a given pattern (the array of S/US characters) associated with the presence/absence of repulsive strain in both t-H and μ-H of each derivative entails a positive or negative sign of $\Delta E^\circ_{\text{t-H}-\mu\text{-H}}$. The information reported in Table 5 is also in good correlation with the trend of E_{SOMO} of reduced species, reported in Table S6. E_{SOMO} proves in this case to be a reliable computational indicator of the redox potential trend associated with the species under study.

Table 5. Strain Pattern Related to Some Key Species Described above in the Text[a]

	μ-H		t-H		
compound	$Fe^{II}Fe^{II}$	$Fe^{II}Fe^{I}$	$Fe^{II}Fe^{II}$	$Fe^{II}Fe^{I}$	$\Delta E^\circ_{\text{t-H}-\mu\text{-H}}$
V/**V'**	US	US	US	US	>0
VI/**VI'**	S	US	S	S	<0
$[\mathbf{V(CO)}]^+$	US	US	US	US	>0
$[\mathbf{VI(CO)}]^+$	S	US	S	US	>0
$[\mathbf{V/V'(PMe_3)}]^+$	US	US	US	US	>0
$[\mathbf{VI'(PMe_3)}]^+$	S	US	US	US	<0
$[\mathbf{V(NHC)}]^+$	US	US	US	US	>0
$[\mathbf{VI(NHC)}]^+$	S	US	US	US	<0

[a]"S" stands for "strained molecule", and "US" stands for " unstrained molecule".

In light of the literature reporting that NHC and PMe_3 have been previously incorporated in diiron dithiolates modeling [FeFe]-H_2ase,[25,26,48] derivatives equipped with such ligands in the Fe apical position ($[\mathbf{VI'(PMe_3)}]^+$ and $[\mathbf{VI(NHC)}]^+$) could be potential candidates for the synthesis of new biomimetic compounds.

DOI: 10.1021/acs.inorgchem.5b01495
Inorg. Chem. 2015, 54, 9529−9542

In Scheme 3, all results presented and discussed in section B are summarized.

Scheme 3. Effects of Y Variations on $\Delta E^{\circ}_{\text{t-H}-\mu\text{-H}}$ (Also Designated as ΔE° for Simplicity) and Results Rationalization

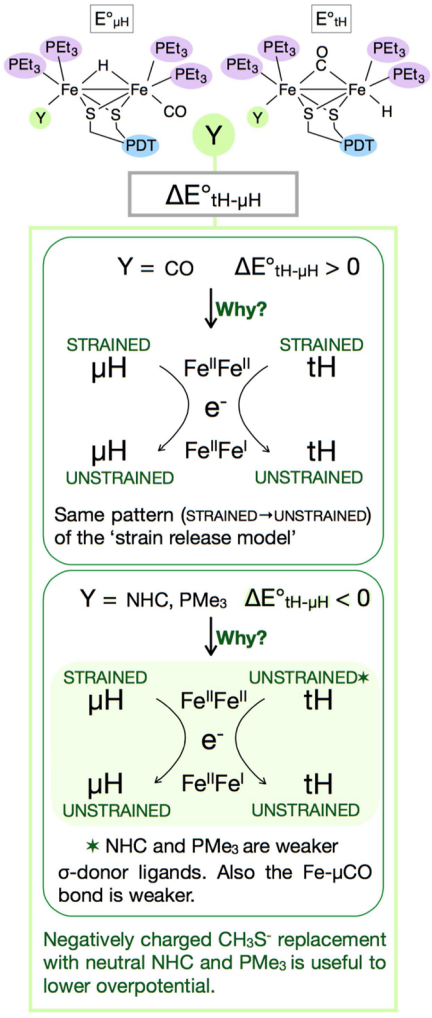

C. Effect of Protonating Apical CH_3S^-. Further, we investigated the possibility of altering $\Delta E^{\circ}_{\text{t-H}-\mu\text{-H}}$ by decreasing the electron-donor character of the CH_3S^- group by protonating the S atom (which could mimic the electron-attracting character of the CO group and the presence of the cubane cluster). Such an effect has been tested on a set of computational models of the active site of [FeFe]-H_2ase (here named [**Hyd X**]). Both dithiolate straps adt and pdt have been considered, a comparison anyway useful for the purposes of the present study, although the issue of the real identity of the X element in $^-SCH_2XCH_2S^-$ has been finally resolved in favor of nitrogen.[8] The presence of CH_3SH in place of the anionic CH_3S^- leads to an increase of $\Delta E^{\circ}_{\text{t-H}-\mu\text{-H}}$ by more than 300 mV in the model featuring pdt, while the augment is more limited in the case of the adt form (Table 6). An easier reduction of the t-H form fits well with the literature, which describes a scenario in which enzyme catalysis is characterized, among other factors, also by kinetic stabilization of the hydride in the terminal position at Fe_d. The t-H-to-μ-H rearrangement, active in all biomimetic compounds, is hindered in the enzyme through

Table 6. $\Delta E^{\circ}_{\text{t-H}-\mu\text{-H}}$ Associated with the Fe_2 Subunit of the H-Cluster (Truncated at the Cysteinyl Thiolate)[a]

compound	$\Delta E^{\circ}_{\text{t-H}-\mu\text{-H}}$ (mV)
$[\mathbf{Hyd\ I}]^{2-}$	152
$[\mathbf{Hyd\ II}]^{2-}$	222
$[\mathbf{Hyd\ III}]^{-}$	478
$[\mathbf{Hyd\ IV}]^{-}$	307

[a] $[\mathbf{Hyd\ I}]^{2-}$ = $[HFe_2(pdt)(CO)_3(CN)_2(SCH_3)]^{2-}$, $[\mathbf{Hyd\ II}]^{2-}$ = $[HFe_2(adt)(CO)_3(CN)_2(SCH_3)]^{2-}$, $[\mathbf{Hyd\ III}]^{-}$ = $[HFe_2(pdt)(CO)_3(CN)_2(SCH_3)]^{-}$, and $[\mathbf{Hyd\ IV}]^{-}$ = $[HFe_2(adt)(CO)_3(CN)_2(SCH_3)]^{-}$.

interaction between the ligand CN^- and a conserved lysine.[14,27] In these conditions, the formation of a μ-H isomer would bring a less favored reductive event, probably impairing the catalytic efficiency.

D. Effect of Replacing pdt with adt (and Protonated Forms Hadt).[55] The redox potentials of $[\mathbf{VI(NHC)}]^+$ for both hydride forms (−2.513 V for μ-H and −2.557 V for t-H vs Fc^+/Fc, CH_2Cl_2) still reveal overpotential (although less than that of CH_3S^--based species), as expected because of the large number of donor ligands coordinated to the Fe_2 center. A possible mitigation of this effect has been obtained by replacing pdt with adt.

Indeed, the central amine of adt derivatives can be protonated in solutions by acids thus bearing an extra net positive charge in diiron dithiolate.[22] However, because hydride species bearing nonprotonated adt are also detected in the CH_2Cl_2 solution, $\Delta E^{\circ}_{\text{t-H}-\mu\text{-H}}$ has been computed also for some analogues of Table 1 in which pdt has been replaced with neutral azadithiolate (see Table S7).

Moreover, two derivatives experimentally synthesized, $[HFe_2(pdt)(CO)_2(dppv)_2]^+$ and $[HFe_2(pdt)(CO)_4(PMe_3)_2]^{+}$[25] ($\Delta E^{\circ}_{\text{t-H}-\mu\text{-H}}$ = 188 mV), have also been considered. These last two sets of calculations have served mainly as benchmarks for the present investigation (see the Computational Methods for $[HFe_2(pdt)(CO)_2(dppv)_2]^+$).

The obtained values confirm the same qualitative trend as that observed for pdt-based derivatives, even if a negative $\Delta E^{\circ}_{\text{t-H}-\mu\text{-H}}$ cannot be observed, probably because of a NH−Fe stabilizing interaction, which selectively favors t-H (see below the discussion on Hadt derivatives for further details).

When switching to protonated (Hadt) derivatives, it can be noted that $[\mathbf{VI(Hadt)(NHC)}]^{2+}$ shows, as expected, less negative E° values both in μ-H (−1.797 V vs Fc^+/Fc, CH_2Cl_2) and in t-H (−1.117 V vs Fc^+/Fc, CH_2Cl_2). Regrettably, yet, this result goes to the detriment of the desired $\Delta E^{\circ}_{\text{t-H}-\mu\text{-H}}$ sign, as is observable in Table 7. The reasons for that can be found in a strong intramolecular NH_2^+−HFe interaction (dihydrogen bonding), which selectively favors t-H versus μ-H, a feature recently illustrated also at the solid state in $[Fe_2(Hadt)(CO)_2(dppv)_2]^{2+}$ by Rauchfuss' group.[22]

However, the strength of this interaction and also the doubly positive charge of $[\mathbf{VI(Hadt)(NHC)}]^{2+}$ could be overestimated by the previous calculations because of the absence of explicit counterions such as BF_4^-, which could be present near the electrode surface in buffers used in a real cyclic voltammetry experiment. In addition, it has been reported that BF_4^- ions can alter a delicately balanced equilibrium existing between N- and Fe-protonated isomers.[22] The results show that adding explicit BF_4^- ions in the simulation brings about an 8-fold decrease of $\Delta E^{\circ}_{\text{t-H}-\mu\text{-H}}$ with respect to the isolated bis-cation (see Table 7),

DOI: 10.1021/acs.inorgchem.5b01495
Inorg. Chem. 2015, 54, 9529−9542

Table 7. Standard Reduction Potential Gap ($\Delta E^\circ_{\text{t-H}-\mu\text{-H}}$ in mV) of Derivatives Containing Hadt as a Dithiolate Strap

compound	$\Delta E^\circ_{\text{t-H}-\mu\text{-H}}$ (mV)
$[V(Hadt)]^+$	576
$[VI(Hadt)]^+$	399
$[VI(Hadt)(NHC)]^{2+}$	680
$[V(Hadt)(NHC)]^{2+}\cdot 2BF_4^-$	218
$[VI(Hadt)(NHC)]^{2+}\cdot 2BF_4^-$	84
$[HFe_2(Hadt)(CO)(dppv)_2(CH_3S)]^+$	455
$[HFe_2(pdt)(CO)(dppv)_2(CH_3S)]^a$	124

[a]This is the only pdt-based species reported as a reference for discussing the "Hadt versus pdt" effect in a derivative simultaneously bearing the dppv chelate and an apical CH_3S^- (see the text).

which definitively points to a strong effect of the molecular charge on the redox gap. Although marked, however, the charge effect is not sufficient in this case to observe a μ-H reduction favored over that of t-H. It is worth recalling, nonetheless, that 84 mV (1.9 kcal mol^{-1}) is a value essentially very close to the precision limit of the employed computational method, thus indicating that a species may exist with t-H and μ-H with roughly the same reduction potential.

The emerging scenario reveals that the amount of negative charge that is pushed into the diiron system is able to significantly affect $\Delta E^\circ_{\text{t-H}-\mu\text{-H}}$. This aspect is to be taken into appropriate consideration for fine-tuning a parameter, which could be relevant in the design of new catalysts. It becomes thus clear that a problem arises when pursuing the alternative strategy that we have herein explored, and that is thus worth recalling at this point: the design of a model species characterized by $\Delta E^\circ_{\text{t-H}-\mu\text{-H}} < 0$. This result is indeed achievable but only by very electron-rich derivatives, thus obviously characterized by reduction overpotential. Any attempt that we made to decrease E° entails a $\Delta E^\circ_{\text{t-H}-\mu\text{-H}}$ shift toward more positive values. This point is confirmed also upon a comparison of $[HFe_2(Hadt)(CO)(dppv)_2(CH_3S^-)]^+$ versus $[HFe_2(pdt)(CO)(dppv)_2(CH_3S^-)]$ (see Table 7), in which we probed the effect of replacing a CO with CH_3S^- in Hadt and pdt derivatives, experimentally synthesized. CH_3S^- causes a $\Delta E^\circ_{\text{t-H}-\mu\text{-H}}$ shift toward less positive values (from 216 to 124 mV) in the pdt species, which is compatible with the role we described above for such a ligand. The case simulation of $[HFe_2(pdt)(CO)(dppv)_2(CH_3S^-)]$ is also interesting in that it allows one to call back the importance of the "repulsive strain factor", as we defined it previously: this derivative has the same overall charge as **VI**/**VI′**, and all of these species share a common CH_3S^- bound at Fe_p.

Despite all similarities, however, $\Delta E^\circ_{\text{t-H}-\mu\text{-H}}$ is clearly positive in $[HFe_2(pdt)(CO)(dppv)_2(CH_3S^-)]$ and negative in **VI** (strongly negative in **VI′**), a result that we explain by the different intramolecular repulsive bumps that characterize these derivatives. In fact, phenyl rings of the dppv chelate can be observed to take on stabilization of T-shape orientations, at both the computational and X-ray crystallography level.[22] Also, in this case, however, upon switching to the Hadt species, a strong shift of $\Delta E^\circ_{\text{t-H}-\mu\text{-H}}$ is observed, as in all preceding cases, demonstrating (once again) how an unequivocal connection exists between absolute redox potentials and their gap in t-H versus μ-H isomers. A compromise between the reduction overpotential and the desired $\Delta E^\circ_{\text{t-H}-\mu\text{-H}}$ is therefore a probable key to design more efficient electrocatalysts. In such a sense, the tiny value computed for the redox gap value found for $[VI(Hadt)(NHC)]^{2+}\cdot 2BF_4^-$ could be considered stimulating. In Scheme 4, all results presented and discussed in section D are summarized.

Scheme 4. Effects of Variations of the xdt Strap on $\Delta E^\circ_{\text{t-H}-\mu\text{-H}}$ (Also Designated as ΔE° for Simplicity) and Results Rationalization

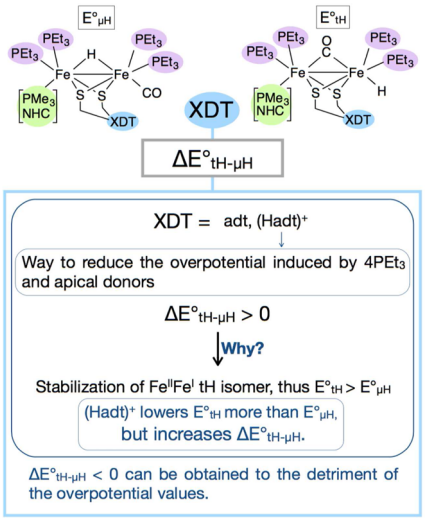

E. Energetics of H_2 Formation in VI/VI′ (4-PEt$_3$). As shown, **VI** has featured interesting redox properties, as emerged by the peculiar reductive behavior of its hydrido isomers. As a result, we have further characterized **VI** by evaluating the thermodynamics associated with the four elementary steps forming the minimal HER pathway (Scheme 5): protonation, reduction, protonation, and H_2 release. The term "minimal" refers to the fact that the second reduction equivalent (necessary for HER to be catalytic) has not been considered here.

Scheme 5 shows that all steps leading to dihydrogen production (at the $Fe^{II}Fe^I$ state of a diiron cluster) are exergonic for both hydrides. As aforementioned, being that the μ-H's of **VI** and **VI′** are very close in energy, the thermodynamics of HER has been evaluated for both isomers. The higher affinity for protons in the Fe^IFe^I state resulted from their association with the Fe−Fe bond region, perfectly in line with previous literature showing that the highest occupied molecular orbital of these states is localized in close proximity to the Fe−Fe bond. Proton affinities have also been calculated for **V** hydrides, with the aim of verifying whether the Me versus Et replacement could influence basic properties besides the redox behavior of the investigated derivatives. Our results (not shown) demonstrate that this is not the case because **V** versus **VI**/**VI′** affinities differ by less than 1 kcal mol^{-1}.

More relevant is the observation that the isomer featuring a rotated geometry of Fe_d is the most stable form at the Fe^IFe^I unprotonated state. The importance resides in the fact that this state/geometry is exactly the one associated with the H_{red} state of the [FeFe]-H_2ase, which actually features a rotated or inverted square-pyramidal geometry at Fe_d, which thus has a vacant (apical) coordination position. Another possibility, still compatible with the available data on H_{red}, is that the axial position at Fe_d is not vacant but occupied by a H ligand, in a diamagnetic $Fe^{II}Fe^{II}$-H species.

DOI: 10.1021/acs.inorgchem.5b01495
Inorg. Chem. 2015, 54, 9529−9542

Scheme 5. Thermodynamic Profile Associated with HER (kcal mol^{-1}) by the VI/VI′ System[a]

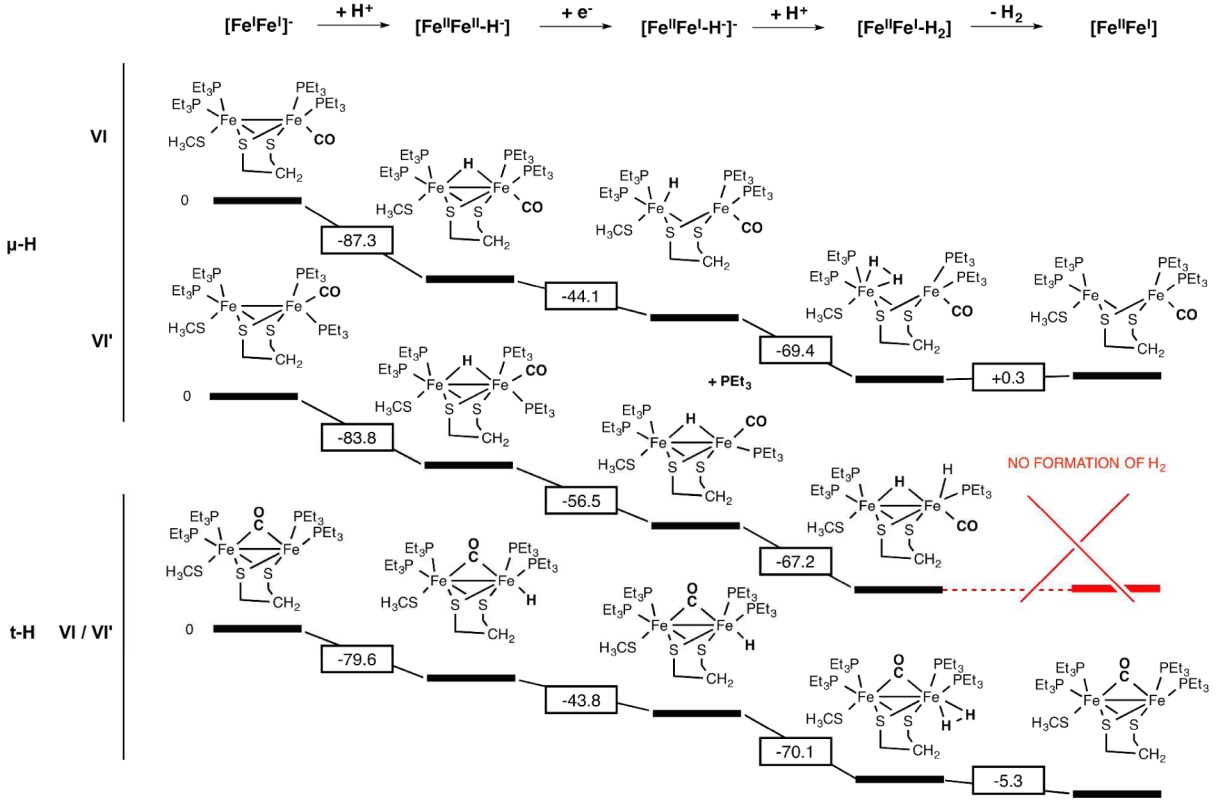

[a] Both μ-H of **VI** and **VI′** have been considered, whereas t-H is the same in both **VI** or **VI′**. Final reduction of the free Fe^{II}Fe^{I} state, which is invoked to close the catalytic cycle, has been omitted.

A rotated isomer of synthetic analogues of the enzyme has been sought-after for a long time (because the most stable form always resulted in the unrotated/eclipsed isomer) until recently because two groups have detected a fully inverted geometry at a single Fe of diiron dithiolates (both adt and pdt) containing bis-P chelate ligands.[36,56]

It is worth highlighting, however, that in these cases the target was accomplished by a subtle balance between steric effects, coordination asymmetry, and weak intramolecular agostic interactions, hindering isomerization of rotated to eclipsed species.[36,56] All of that cannot occur in the enzyme, though. In contrast, the stabilizing effect could be ascribed here to electronic factors such as the σ-donor properties of CH_3S^-, analogous to what previously proposed by Bruschi et al., highlighting the importance of the apical cysteine of the enzyme cofactor.[57]

To confirm the role possibly played by CH_3S^-, we performed a comparative speciation study of isomer **VI** versus [**VI**(**CO**)]$^+$: the results are illustrated in Figure 5 and demonstrate undoubtedly the effect of the apical S ligand in stabilizing the rotated isomer.

It is interesting at this point to ascertain whether the stabilization of rotated forms arises only from the CH_3S^- versus CO effect or whether the presence of Et_3P versus Me_3P may have some influence. Therefore, the same speciation has been performed for **V** versus [**V**(**CO**)]$^+$: remarkably, **V** still has the rotated isomer as the most stable form, but the energy difference between rotated and unrotated drops to 2.4 kcal mol^{-1} (vs 6.3 kcal mol^{-1} observed in **VI**). It can thus be concluded that steric repulsions play a role also as far as stabilization of rotated Fe^{I}Fe^{I} isomers is concerned.

The second step of HER, i.e., reduction of protonated forms, has been the subject of the discussion presented above. The third step, namely, the second protonation (of reduced forms), is energetically very similar in both isomers and thus is not worthy of further discussion.

As for the H_2 formation−release steps (see Scheme 5, on the right), it is worth noting that, in μ-H, the formation of H_2 occurs at Fe_p, while in t-H, it is formed at Fe_d. In the first case, H_2 has a strong σ-donor trans-oriented to it, while in the latter case, the ligand trans to H_2 is the strongest π-acceptor (i.e., the Fe−Fe bridging CO). The different nature of ligands trans-oriented with respect to the exiting H_2 and CO could be related to the different thermodynamics of H_2 formation in t-H (exergonic process) versus μ-H (quasi-equilibrium process). Fe_p is particularly electron-rich because of the presence of CH_3S^-, thus implying a significant π-back-donation from Fe_p into the H_2 σ^* orbital. Fe_d is instead electron-poorer than Fe_p because of the presence of the bridging CO trans-oriented to the H_2 ligand, entailing a diminished back-donation into the H_2 antibonding orbital. Also, the H−H and Fe−H distances in the Fe−H_2 moiety of t-H and μ-H are compatible with the preceding considerations. In fact, in t-H, the H−H and Fe−H distances are 0.845 and 1.674 Å, respectively, because of lower back-donation, caused by trans CO, from Fe into the H_2 σ^* orbital. Conversely, in μ-H, the H−H and Fe−H distances are 0.894 and 1.591 Å (avg), respectively. This is conceivably due to larger back-donation, triggered by trans CH_3S^-, from Fe into the antibonding H_2 orbitals, thus indicating in this case a H_2 ligand that appears more tightly bound to Fe and thus less activated for release. Besides well correlating to the thermodynamics of the H_2 release step from **VI**, the described

DOI: 10.1021/acs.inorgchem.5b01495
Inorg. Chem. 2015, 54, 9529−9542

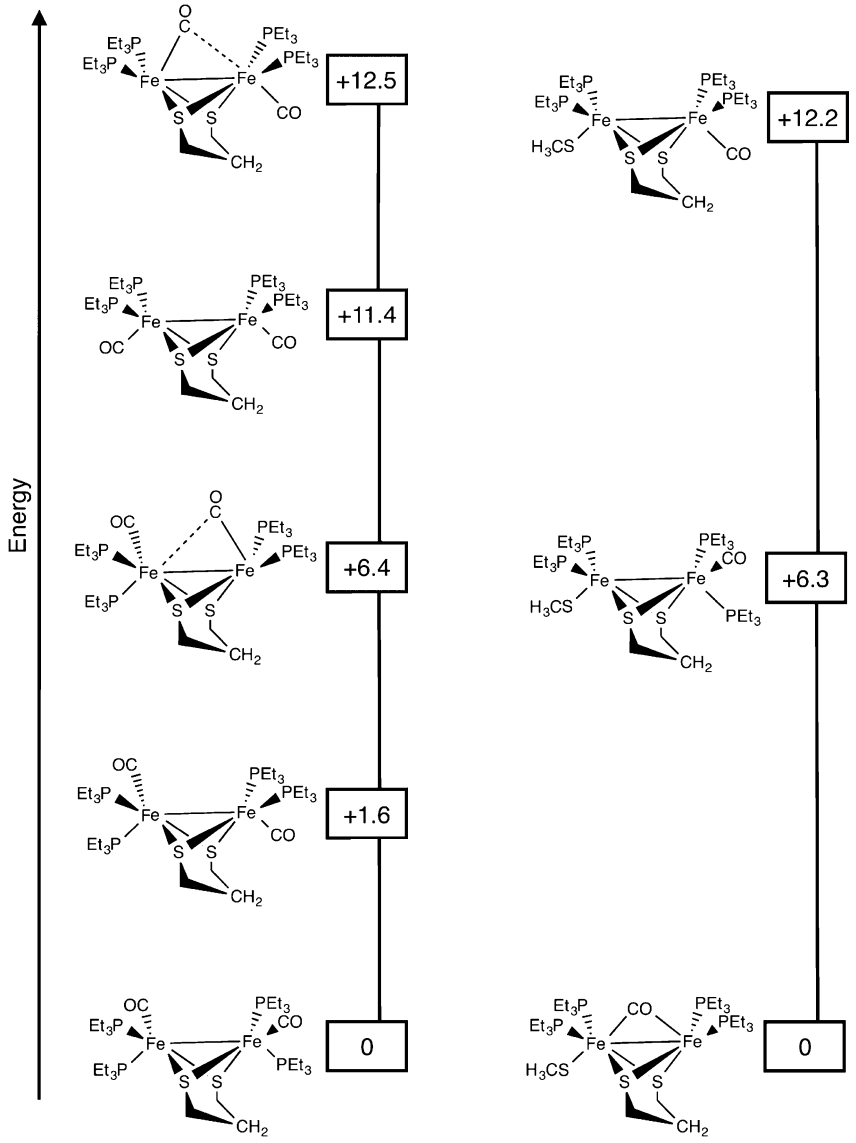

Figure 5. Relative stability (kcal mol^{-1}) of unprotonated forms related to **VI** and **VI(CO)**.

scenario provides a clear clue on which of the two contributions describing the coordination model of H_2 to a metal center is dominant in the investigated case. The π-back-donation into the H_2 antibonding orbital is responsible for coordination of the ligand to metal, and as if one invoked σ-donation from H_2 to Fe, reverse (and wrong) predictions would be cast: electron-poor Fe (as in t-H) should release H_2 endergonically, and electron-rich Fe (as in μ-H) should behave oppositely.

Finally, it is worth pointing out that H_2 formation−release cannot intrinsically occur via **VI′** μ-H mediation because, due to the loss of phosphine upon the first reduction, Fe_d would remain coordinatively unsaturated.

■ CONCLUSIONS

The results of the present investigation can be summarized as follows:

(i) Increasing the number of electron donors on the protonated diiron dithiolates $[HFe_2(xdt)(PR_3)_n(CO)_{5-n}X]$ (n = 0, 2, 4; R = H, Me, Et; X = CH_3S^-, PMe_3, NHC = 1,3-dimethylimidazol-2-ylidene; xdt = adt, pdt; adt = azadithiolate; pdt = propanedithiolate) is predicted to alter $\Delta E^\circ_{t\text{-}H-\mu\text{-}H}$ in a nonlinear way, up to a substitution extent of the diiron core at which subtle steric factors come into play (vide infra) entailing a surprising modulation of the redox gap. Otherwise stated, simply replacing CO with "donors" has a steric effect, provided that R of tertiary phosphines is bulkier than Me. It is worth noting that, even though PMe_3 and PEt_3 are usually considered to be compact, when many are installed on Fe_2, the result is crowding.

(ii) Intramolecular steric repulsions among bulky R_3P ligands of *highly substituted* ($Fe_2(PR_3)_4$) diiron dithiolates cause an unsuspected effect on $\Delta E^\circ_{t\text{-}H-\mu\text{-}H}$: an inversion of its sign, exactly the target of the present investigation. Variation upon reduction of the structural and energetic parameters shows that such a result is due to a steric strain (or destabilization), which affects differently the μ-H and t-H isomeric forms. Thus, μ-H of highly substituted derivatives with bulky R_3P in their oxidated $Fe^{II}Fe^{II}$ state is unstable toward reduction, compared to analogues with R of smaller size. The intramolecular strain thus generated can be released upon one-electron reduction in two ways depending on which one of the two rotational stereoisomers of μ-H is being reduced. When μ-H **VI** [4-PEt_3;

DOI: 10.1021/acs.inorgchem.5b01495
Inorg. Chem. 2015, 54, 9529−9542

coordination environment of Fe_d: $(CO)_{ap}-Fe-(PEt_3)_{2ba-ba}$] is reduced, Fe−Fe and one of the two Fe−H bonds are broken, whereas if reduction occurs on μ-H **VI′** [4-PEt_3; coordination environment of Fe_d: $(PEt_3)_{ap}-Fe-(CO)_{ba}(PEt_3)_{ba}$], then a Fe−$PEt_3$ bond dissociation is observed. The main point is that only μ-H shows release of the intramolecular strain because in t-H, a FeFe bridging CO, which is strong π-acceptor and trans-oriented to two strong σ-donors, forms two strong Fe−(CO)−Fe bonds, preventing the two L_3Fe moieties from moving away from each other. Therefore, t-H of electron-rich species simultaneously bearing bulky R_3P ligands cannot release the intramolecular strain, whereas μ-H does. This justifies the inversion of the $\Delta E^\circ_{\text{t-H}-\mu\text{-H}}$ sign observed in **VI**-like systems.

(iii) The role of the apical CH_3S^- (or other σ-donors, vide infra) appears relevant because this ligand, trans-oriented to a bridging CO, is important to maintain terminal hydrides in a "strained" or "energetically unstable" configuration, at both oxidized and reduced states (whereas in bridging hydrides the strain is relaxed upon one-electron reduction). This implies that the $Fe_2(SR)_2$ scaffold has to be 5-substituted, which does not appear to be a straightforward task from a synthetic standpoint. Noticeably, Rauchfuss et al. have recently synthesized and characterized the dihydrido complex [(*term*-H)(μ-H)Fe_2(pdt)-(CO)$(dppv)_2$], which contains up to six donor groups [in addition to the $(SR)_2$ of the pdt strap].[58]

(iv) In the case of neutrally charged σ-donors, less strong than the apical RS^- (such as NHC), our results again show a $\Delta E^\circ_{\text{t-H}-\mu\text{-H}} < 0$, although t-H's of such derivatives show structural parameters indicating either P−Fe or "Fe−Fe/Fe-H" bond breaking. Justification of such a result requires therefore generalization of the model based on the strain presence/absence and on how/if it can be released upon reduction. The general factor underlying the positivity or negativity of $\Delta E^\circ_{\text{t-H}-\mu\text{-H}}$ is the similarity or diversity of the reductive behavior by t-H versus μ-H of a given species. Therefore, in the case of species with NHC and PMe_3, their t-H is strain-free already at the oxidized state because two such ligands are not able to make sufficiently strong Fe−CO bonds, which would preserve the "unstable" configuration. By contrast, μ-H of the same species is affected by intramolecular repulsion at the oxidized state, reduction of which allows alleviation. This implies that the behavior of t-H versus μ-H is once again different, although according to another pattern compared to that emerged in CH_3S^--based species. It is worth pointing out that the possibility of replacing the anionic CH_3S^- with neutrally charged σ-donors is a relevant factor because it favors the lowering of the reduction overpotentials (see also item v).

(v) Reducing the overall charge of the diiron dithiolates by, for instance, replacing neutral pdt with nitrogen-containing linkers that are susceptible to being protonated by acids, tends to favor t-H reduction over μ-H ($\Delta E^\circ_{\text{t-H}-\mu\text{-H}}$ is shifted toward more positive values). The same effect is observed when calculating $\Delta E^\circ_{\text{t-H}-\mu\text{-H}}$ after protonation of the apical CH_3S^- in models of the diiron core of the enzyme active site. These observations, along with the necessity of incorporating a large number of donor ligands in the diiron dithiolate, before the "repulsive strain effect" pops up, implies that nonnegligible overpotentials are to be taken into consideration. Therefore, a compromise that can balance the "overpotential versus $\Delta E^\circ_{\text{t-H}-\mu\text{-H}}$" competition has to be pursued.

(vi) Other peculiar features that emerged about 4-PEt_3-based systems, possibly relevant for the design of new biomimetic compounds, are as foolows: (i) t-H is thermodynamically favored over μ-H at the $Fe^{II}Fe^{II}$ state; (ii) the $Fe^{I}Fe^{I}$ state before protonation features a rotated (inverted) structure at Fe_d, which is reminiscent of the same coordination geometry that such Fe maintains in the H-cluster during the enzyme turnover. Both aspects (i) and (ii) are connected with the strong donor properties of the apical ligand at Fe_p.

■ ASSOCIATED CONTENT

Supporting Information

The Supporting Information is available free of charge on the ACS Publications website at DOI: 10.1021/acs.inorgchem.5b01495.

Table and figures of converged SCF energies, $\Delta E^\circ_{\text{t-H}-\mu\text{-H}}$, calculated at different levels of theory for [HFe_2(pdt)-$(CO)_2(dppv)_2$]$^+$, absolute and relative (vs Fc^+/Fc) values of standard reduction potentials, Mulliken charges, FMO analysis, isosurface plots of the lowest unoccupied molecular orbital of the $Fe^{II}Fe^{II}$ state and the SOMO of $Fe^{II}Fe^{I}$ state, spin densities and additional discussion on the partial charges and spin densities (PDF)

■ AUTHOR INFORMATION

Corresponding Author

*E-mail: giuseppe.zampella@unimib.it.

Notes

The authors declare no competing financial interest.

■ ACKNOWLEDGMENTS

We are grateful to the PRIN for financial support (project 2010M2ARJ_010). We would like to thank Tom Rauchfuss, Philippe Schollhammer, and Jean Talarmin for valuable exchanges of ideas.

■ REFERENCES

(1) Lubitz, W.; Tumas, W. *Chem. Rev.* **2007**, *107*, 3900−3903.
(2) Fontecilla-Camps, J. C.; Volbeda, A.; Cavazza, C.; Nicolet, Y. *Chem. Rev.* **2007**, *107*, 4273−4303.
(3) Tard, C.; Pickett, C. J. *Chem. Rev.* **2009**, *109*, 2245−2274.
(4) Peters, J. W.; Lanzilotta, W. N.; Lemon, B. J.; Seefeldt, L. C. *Science* **1998**, *282*, 1853−1858.
(5) Nicolet, Y.; Piras, C.; Legrand, P.; Hatchikian, C. E.; Fontecilla-Camps, J. C. *Structure* **1999**, *7*, 13−23.
(6) Nicolet, Y.; de Lacey, A. L.; Vernède, X.; Fernandez, V. M.; Hatchikian, E. C.; Fontecilla-Camps, J. C. *J. Am. Chem. Soc.* **2001**, *123*, 1596−1601.
(7) Shima, S.; Pilak, O.; Vogt, S.; Schick, M.; Stagni, M. S.; Meyer-Klaucke, W.; Warkentin, E.; Thauer, R. K.; Ermler, U. *Science* **2008**, *321*, 572−575.
(8) Berggren, G.; Adamska, A.; Lambertz, C.; Simmons, T. R.; Esselborn, J.; Atta, M.; Gambarelli, S.; Mouesca, J.-M.; Reijerse, E.; Lubitz, W.; Happe, T.; Artero, V.; Fontecave, M. *Nature* **2013**, *499*, 66−69.
(9) Nicolet, Y.; Lemon, B. J.; Fontecilla-Camps, J. C.; Peters, J. W. *Trends Biochem. Sci.* **2000**, *25*, 138−143.
(10) Bruschi, M.; Greco, C.; Kaukonen, M.; Fantucci, P.; Ryde, U.; De Gioia, L. *Angew. Chem., Int. Ed.* **2009**, *48*, 3503−3506.
(11) Silakov, A.; Wenk, B.; Reijerse, E.; Lubitz, W. *Phys. Chem. Chem. Phys.* **2009**, *11*, 6592−6599.
(12) Razavet, M.; Borg, S. J.; George, S. J.; Best, S. P.; Fairhurst, S. A.; Pickett, C. J. *Chem. Commun.* **2002**, *7*, 700−701.
(13) Chong, D.; Georgakaki, I. P.; Mejia-Rodriguez, R.; Sanabria-Chinchilla, J.; Soriaga, M. P.; Darensbourg, M. Y. *Dalton Trans.* **2003**, *21*, 4158−4163.

DOI: 10.1021/acs.inorgchem.5b01495
Inorg. Chem. 2015, 54, 9529−9542

(14) Gloaguen, F.; Lawrence, J. D.; Rauchfuss, T. B. *J. Am. Chem. Soc.* **2001**, *123*, 9476−9477.
(15) Gloaguen, F.; Lawrence, J. D.; Rauchfuss, T. B.; Bénard, M.; Rohmer, M.-M. *Inorg. Chem.* **2002**, *41*, 6573−6582.
(16) Zhao, X.; Georgakaki, I. P.; Miller, M. L.; Yarbrough, J. C.; Darensbourg, M. Y. *J. Am. Chem. Soc.* **2001**, *123*, 9710−9711.
(17) Knörzer, P.; Silakov, A.; Foster, C. E.; Armstrong, F. A.; Lubitz, W.; Happe, T. *J. Biol. Chem.* **2012**, *287*, 1489−1499.
(18) Tschierlei, S.; Ott, S.; Lomoth, R. *Energy Environ. Sci.* **2011**, *4*, 2340−2352.
(19) Zampella, G.; Fantucci, P.; De Gioia, L. *Chem. Commun.* **2009**, *46*, 8824−8826.
(20) Finkelmann, A. R.; Stiebritz, M. T.; Reiher, M. *Chem. Sci.* **2014**, *5*, 215−221.
(21) Ezzaher, S.; Capon, J. F.; Gloaguen, F.; Pétillon, F. Y.; Schollhammer, P.; Talarmin, J.; Pichon, R.; Kervarec, N. *Inorg. Chem.* **2007**, *46*, 3426−3428.
(22) Van der Vlugt, J. I.; Rauchfuss, T. B.; Whaley, C. M.; Wilson, S. R. *J. Am. Chem. Soc.* **2005**, *127*, 16012−16013.
(23) Barton, B. E.; Rauchfuss, T. B. *Inorg. Chem.* **2008**, *47*, 2261−2263.
(24) Carroll, M. E.; Barton, B. E.; Rauchfuss, T. B.; Carroll, P. J. *J. Am. Chem. Soc.* **2012**, *134*, 18843−18852.
(25) Jablonskytė, A.; Wright, J. A.; Fairhurst, S. A.; Peck, J. N. T.; Ibrahim, S. K.; Oganesyan, V. S.; Pickett, C. J. *J. Am. Chem. Soc.* **2011**, *133*, 18606−18609.
(26) Zaffaroni, R.; Rauchfuss, T. B.; Gray, D. L.; De Gioia, L.; Zampella, G. *J. Am. Chem. Soc.* **2012**, *134*, 19260−19269.
(27) Gloaguen, F.; Rauchfuss, T. B. *Chem. Soc. Rev.* **2009**, *38*, 100−108.
(28) Lubitz, W.; Ogata, H.; Rüdiger, O.; Reijerse, E. *Chem. Rev.* **2014**, *114*, 4081−4148.
(29) Hoffman, B. M.; Lukoyanov, D.; Dean, D. R.; Seefeldt, L. C. *Acc. Chem. Res.* **2013**, *46*, 587−595.
(30) Furche, F.; Ahlrichs, R.; Hättig, C.; Klopper, W.; Sierka, M.; Weigend, F. *Wiley Interdiscip. Rev. Comput. Mol. Sci.* **2014**, *4*, 91−100.
(31) Eichkorn, K.; Weigend, F.; Treutler, O.; Ahlrichs, R. *Theor. Chem. Acc.* **1997**, *97*, 119−124.
(32) Schäfer, A.; Huber, C.; Ahlrichs, R. *J. Chem. Phys.* **1994**, *100*, 5829−5835.
(33) Perdew, J. P. *Phys. Rev. B: Condens. Matter Mater. Phys.* **1986**, *33*, 8822−8824.
(34) Becke, A. D. *Phys. Rev. A: At., Mol., Opt. Phys.* **1988**, *38*, 3098−3100.
(35) Bruschi, M.; Greco, C.; Fantucci, P.; De Gioia, L. *Inorg. Chem.* **2008**, *47*, 6056−6071.
(36) Munery, S.; Capon, J. F.; De Gioia, L.; Elleouet, C.; Greco, C.; Pétillon, F. Y.; Schollhammer, P.; Talarmin, J.; Zampella, G. *Chem. - Eur. J.* **2013**, *19*, 15458−15461.
(37) Miyake, T.; Bruschi, M.; Cosentino, U.; Baffert, C.; Fourmond, V.; Léger, C.; Moro, G.; De Gioia, L.; Greco, C. *JBIC, J. Biol. Inorg. Chem.* **2013**, *18*, 693−700.
(38) Zampella, G.; Fantucci, P.; De Gioia, L. *J. Am. Chem. Soc.* **2009**, *131*, 10909−10917.
(39) Becke, A. D. *J. Chem. Phys.* **1993**, *98*, 5648−5652.
(40) Lee, C.; Yang, W.; Parr, R. G. *Phys. Rev. B: Condens. Matter Mater. Phys.* **1988**, *37*, 785−789.
(41) Li, J.; Fisher, C. L.; Chen, J. L.; Bashford, D.; Noodleman, L. *Inorg. Chem.* **1996**, *35*, 4694−4702.
(42) Roy, L. E.; Batista, E. R.; Hay, P. J. *Inorg. Chem.* **2008**, *47*, 9228−9237.
(43) Jensen, F. *Introduction to Computational Chemistry*; John Wiley & Sons Ltd.: Chichester, England, 2012.
(44) Klamt, A. *J. Phys. Chem.* **1995**, *99*, 2224−2235.
(45) Klamt, A. *J. Phys. Chem.* **1996**, *100*, 3349−3353.
(46) Song, L. C.; Yang, Z. Y.; Bian, H. Z.; Hu, Q. M. *Organometallics* **2004**, *23*, 3082−3084.
(47) Wang, Z.; Liu, J. H.; He, C. J.; Jiang, S.; Åkermark, B.; Sun, L. C. *J. Organomet. Chem.* **2007**, *692*, 5501−5507.
(48) Capon, J. F.; El Hassnaoui, S.; Gloaguen, F.; Schollhammer, P.; Talarmin, J. *Organometallics* **2005**, *24*, 2020−2022.
(49) Tolman, C. A. *Chem. Rev.* **1977**, *77*, 313−348.
(50) Chatt, J.; Kan, C. T.; Leigh, G. J.; Pickett, C. J.; Stanley, D. R. *J. Chem. Soc., Dalton Trans.* **1980**, *10*, 2032−2038.
(51) Wilkinson, G.; Gillard, R. D.; McCleverty, J. A. *Comprehensive Coordination Chemistry*; Pergamon Press: Oxford, U.K., 1987; Vol. *1*.
(52) Lever, A. B. P. *Inorg. Chem.* **1990**, *29*, 1271−1285.
(53) Henderson, W. A.; Streuli, C. A. *J. Am. Chem. Soc.* **1960**, *82*, 5791−5794.
(54) Aguirre de Carcer, I.; Di Pasquale, A.; Rheingold, A. L.; Heinekey, D. M. *Inorg. Chem.* **2006**, *45*, 8000−8002.
(55) In the case of adt and Hadt derivatives, rotameric forms ap−ba have not been considered because the diequatorial disposition is predicted to be more stable because of an intramolecular interaction occurring between the apical CO at Fe and the HN group of adt.
(56) Wang, W.; Rauchfuss, T. B.; Moore, C. E.; Rheingold, A. L.; De Gioia, L.; Zampella, G. *Chem. - Eur. J.* **2013**, *19*, 15476−15479.
(57) Bruschi, M.; Fantucci, P.; De Gioia, L. *Inorg. Chem.* **2004**, *43*, 3733−3741.
(58) Wang, W.; Rauchfuss, T. B.; Zhu, L.; Zampella, G. *J. Am. Chem. Soc.* **2014**, *136*, 5773−5782.

DOI: 10.1021/acs.inorgchem.5b01495
Inorg. Chem. 2015, 54, 9529−9542